Resonance, chaos and coexistence of attractors in a position dependent mass-driven Duffing-type oscillator

L. A. Hinvi[1,2] · A. A. Koukpémèdji[2,3,4] · V. A. Monwanou[2] · C. H. Miwadinou[2,4,5] · V. Kamdoum Tamba[6] · J. B. Chabi Orou[2]

Abstract

This paper addresses the dynamics of a position-dependent mass-driven Duffing-type oscillator (PDM oscillator) subjected to periodic excitation. The approximate equation of the PDM oscillator is considered to analyze the harmonic oscillations and the possible resonance states. The Amplitudes and frequencies of possible resonances are found by using the harmonic balance method and the multiple scales method. The harmonic resonance, primary resonance, order 3, 5 superharmonic resonances and order 3, 5 subharmonic resonances are obtained. The stability conditions for each of these resonances have also been obtained. Chaotic oscillations, multistability, hysteresis, and coexisting attractors have been found using the bifurcation diagram, the Lyapunov exponents, the phase portraits, and the basin of attraction. The effects of the PDM parameter ξ and of the external excitation have been analyzed. Results obtained by using the approximate equation of the system have been compared to the dynamics obtained with the exact equation of the PDM oscillator. The analytical investigations have been complemented and validated using the numerical simulations.

1 Introduction

In nature, many phenomena are based on nonlinearities. A good knowledge of the laws of nonlinear sciences makes understanding and master of these nonlinear phenomena possible. For this, several researchers have invested the fields such as mathematics, physics, chemistry, finance, epidemiology, aeronautics, engineering, etc. where these nonlinear sciences are applied. A position-dependent mass-driven Duffing-type oscillator (PDM oscillator) is one of these nonlinear systems. For example, the PDM oscillator is used to understand the problems of compositionally graded crystals, quantum dots, quantum liquids, metal clusters, etc. [1–5]. Precisely, quantum-mechanics systems in which the mass (effective) depends on position have received much attention from researchers [6, 7]. The rapid development denote the research carried out on classic problems having a PDM oscillator strongly justifies the interest in PDM oscillators [8–17]. As an example, several authors have worked on the simplest case of a classical PDM oscillator [14, 16, 17]. Recently, Bagchi et al. [6] studied the PDM oscillator whose dynamics were governed by a Duffing oscillator. In their work, they showed that a PDM driven by a Duffing oscillator offered an interesting possibility to analyse the bifurcations, chaos, and regular behaviors of the dynamic system. More recently, in 2020, Roy-Layinde et al. [18] studied the vibrational resonance (VR) of the PDM oscillator

✉ C. H. Miwadinou
clement.miwadinou@imsp-uac.org

[1] Département de Génie Mécanique et Productique, INSTI-Lokossa, (UNSTIM)-Abomey, Abomey, Benin

[2] Laboratoire de Mécanique des Fluides, de la Dynamique Nonlinéaire et de la Modélisation des Systèmes Biologiques (LMFDNMSB), Institut de Mathématiques et de Sciences Physiques, Porto-Novo, Benin

[3] FAST-Natitingou, (UNSTIM)-Abomey, Abomey, Benin

[4] Laboratoire de Physique et Applications, Natitingou, (UNSTIM)-Abomey, Abomey, Benin

[5] Département de Physique, ENS-Natitingou, (UNSTIM)-Abomey, Abomey, Benin

[6] Department of Telecommunication and Network Engineering, IUT-Fotso Victor of Bandjoun, University of Dschang, P.O. Box 134, Bandjoun, Cameroon

using a modulated amplitude force. Through an analytical study and numerical simulations, these authors determined the conditions for appearance of the VR in the PDM oscillator. In practice, during the movement following the addition or removal of particlei the mass changes as a function of time, position or speed or even as a function of the position and the time at that time. In general, variable mass systems are frequently encountered in oceanography, captive satellite dynamics, civil engineering, meteorites, offshore and aerology. Also, they are present in condensed matter systems like heterogeneous semiconductor structures and the inverted potential structure of the ammonia molecule, in particle accretion systems like raindrops, as well as early solar system (the accretion of planets and asteroids) [18]. Thus, from the existing PDM oscillator, the model using Duffing's equation is clearly much more relevant to the richness and complexity of the PDM oscillator's movement than the classical models that exist [6, 18].

From these various previous works, we note that the PDM oscillator modeled by using a Duffing oscillator is a very complex system and can be the seat of many phenomena. We can cite, for example, phenomena such as amplitude jump, hysteresis, nonlinear resonances, chaos, coexistence of attractors, multistability etc. [19–27]. The study of resonance states is very important capital because the amplitude of the vibrations is maximum at the resonance and the energy is proportional to the square of the amplitude of the vibrations [28, 29]. For example, in engineering, anti-resonance systems can be used to store energy with a sudden increase in amplitude at resonance causing a sudden increase in energy and damage the mechanical system. Therefore, clearly nonlinear resonances for the PDM oscillator are very interesting. Today, nonlinear vibration techniques are mostly based on the upper harmonics and the sideband modulation method while approaches to detect nonlinear damage based on nonlinear resonances require even more investigation. For this, knowledge of the relationship between the amplitude of the oscillations and the parameters of the PDM oscillator is essential for a good choice of the frequency and the amplitude of the excitation force to cause a nonlinear resonance effect [30–32].

Finally, multistability is one of the complex phenomena encountered in nonlinear systems. Thus, the dynamics of systems exhibiting this phenomenon of multistability are difficult to analyze. Indeed, for the same value of a parameter of the system for which multistabilization appears, the system is in several states or at several vibration amplitudes, thus making the system difficult to control. On the other hand, bistability reflects the coexistence of two attractors, while megastability designates the coexistence of an infinite number of attractors for the same system [19–21, 33–41]. Several researchers have competed to predict and control multistability due to the complexity of multistable systems.

This explains the many works published over the last decade on this rather interesting subject [19–21, 33–41]. For example, in these different works, several techniques are used by the authors to research, analyze and control the coexistence of attractors and very conclusive results are obtained. As applications, these authors have shown that a great flexibility of the performances of the system is made feasible by the coexistence of different stable states without major changes of parameters.

Our aim in the present work is specifically the study of the harmonics, primary, superharmonic and subharmonic resonances, hysteresis and multistability for the dynamics of the PDM driven by a Duffing oscillator under a periodic excitation. Indeed, the objective of this paper is to deepen and complete the understanding the work [6] in which a the transition to chaos is studied, and the work [17] devoted to the modeling of the dynamics of systems by using the Duffing equation. Thus, the classical PDM system considered here, can be quantified to better understand the individual contribution of each element at the atomic level, and at the quantum levels the energy is a very important parameter for controlling the state of the system. Also, the amplitudes of the vibration of the classical system need to be known because the energy of a system is closely related to the amplitude of vibration of a classical system. Therefore, in this sense, we have found the amplitudes of the harmonic and resonance oscillations of the PDM oscillator. Another very important point of this work is the study of multistability. The study of this phenomenon will allow us to know whether for the same value of each of the parameters of the PDM oscillator, can be in several states at the same time, which will affect the dynamic performance of the PDM. To achieve our goal, we concentrate our studies on the resonance, chaotic oscillations and coexistence of attractors in this PDM oscillator. Due to the high nonlinearity of the problem, we used the approximate PDM oscillator equation and the methods of harmonic balance and of multiple scales to study the possible resonances. Through these studies, we found the effects of the PDM oscillator's parameter and the external excitation force on the nonlinear dynamics of the PDM system.

The paper is structured as follows: Section 2 gives the mathematical modeling of a PDM oscillator while Sect. 3 analyzes the harmonic vibrations. In Sect. 4, we determine the primary resonance while the possible superharmonic and subharmonic resonances obtained by using the method of multiple scales are studied in Sect. 5. Section 6 deals with bifurcation, route to chaos, bistability, coexisting attractors, and hysteresis. Finally, Sect. 7 is devoted to the conclusion.

2 Mathematical model of a position-dependent mass-driven Duffing-type oscillator

We consider in this work a position-dependent mass-driven Duffing-type oscillator whose equation is [6, 17]

$$m(x)\ddot{x} + m'(x)\dot{x}^2 + \alpha\dot{x} + \omega_0^2 x + \beta x^3 = f\cos\omega t, \quad (1)$$

where

$$m(x) = \frac{1}{\sqrt{1 + \xi x^2}}, \quad m'(x) = \frac{dm(x)}{dx},$$

with α being the linear parameter of viscous damping, β the nonlinear Duffing coefficient of stiffness, ξ the PDM oscillator's parameter and $f\cos\omega t$ the external periodic force. When the expression *for m* in Eq. (1) is inserted, the equation of the PDM oscillator becomes

$$\ddot{x} + \sqrt{1 + \xi x^2}\left(\omega_0^2 x + \beta x^3\right) + \alpha\dot{x}\sqrt{1 + \xi x^2}$$
$$- \frac{\xi x\dot{x}^2}{1 + \xi x^2} = f\sqrt{1 + \xi x^2}\cos\omega t. \quad (2)$$

Equation (2) is the classical equation of a Duffing oscillator with forced damping when the mass is constant, i.e. for $\xi = 0$. In order to facilitate the calculations in the search for the resonance states for system, we will consider the approximate equation of the PDM oscillator. Using Taylor's formula and taking $\omega_0^2 = 1$, we can rewrite the dynamic equation of the system as

$$\ddot{x} + x + \alpha\dot{x} + \mu x^2\dot{x} - \xi x\dot{x}^2 + \kappa x^3\dot{x}^2 + \gamma x^3$$
$$+ \lambda x^5 = (1 + \eta x^2)f\cos\omega t, \quad (3)$$

with $\gamma = \beta + \frac{1}{2}\xi$, $\lambda = \frac{\beta\xi}{2}$; $\mu = \frac{1}{2}\alpha\xi$; $\eta = \frac{1}{2}\xi$ and $\kappa = \xi^2$.

3 Harmonic oscillations analysis

In this section, we study the harmonic oscillations of the system. For this, when the fundamental component of the solution and the external excitation have the same frequency, the amplitude of harmonic oscillations can be found using the harmonic balance method. Thus, we express its solutions as [42, 43]

$$x = A\cos(\omega t + \phi) + \psi, \quad (4)$$

where A represents the amplitude of the oscillations and ψ is a constant, with $|\psi| \ll |A|$. Under this condition, inserting Eq. (4) in Eq. (3) and after some algebraic manipulations, we obtain the amplitudes of harmonic oscillations which obey the following equation

$$\left(1 - \omega^2 - \frac{1}{4}\epsilon A^2\omega^2 + \frac{1}{8}\kappa\omega^2 A^4 + \frac{3}{4}\gamma A^2 + \frac{5}{8}\lambda A^4\right)^2 A^2$$
$$+ \left(\alpha + \frac{1}{4}\mu A^2\right)^2 \omega^2 A^2 = f^2\left(1 + \frac{3}{4}\nu A^2\right)^2, \quad (5)$$

with

$$\omega^2 = \frac{\eta Af - \frac{3}{2}\gamma A^2 - \frac{15}{8}\lambda A^4 - 1}{\frac{3}{8}\kappa A^4 - \frac{1}{2}\eta A^2}. \quad (6)$$

We now analyze the behaviors of the amplitude A of the oscillations of the system as a function of the excitation frequency ω, the amplitude f of the external excitation, and the parameter ξ ensuring the dependence on the mass's position. The different results obtained are shown in Figs. 1, 2, 3. Figure 1 shows a comparison between the analytical and numerical results where the black curve is the resonance curve obtained using Eqs. (5) and (6), the blue curve is obtained using the normal model (Eq. (2)) and the red denotes the numerical results obtained from the approximate model (Eq. (3)). The numerical solutions are obtained by solving Eq. (2) (for exact model) and Eq. (3) (for approximate model). To this end, we used the fourth-order Runge–Kutta integration algorithm. We notice through these three curves a good agreement between the three results thus validating the approximate model and the analytical result obtained. Moreover, the analysis of the resonance curve obtained reveals that the resonance is nonlinear and that the system exhibits stable and unstable oscillations amplitudes. Figure 2 represents the effects of the parameters f and ξ on the obtained resonance curve. We note that the resonance amplitude and the resonance frequency increase with f and ξ and this leads to amplitude jump phenomenon. Finally, Fig. 3 shows the evolution of the amplitude A of the oscillations as a function of ξ (Fig. 3a) and of the amplitude of the external
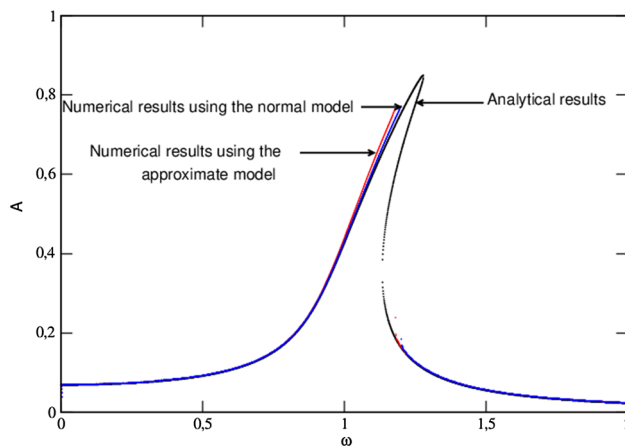

Fig. 1 Comparison between the analytical and the numerical frequency-response curves $A(\omega)$ with $\alpha = 0.07, \beta = 1, \xi = 0.5$, and $f = 0.07$
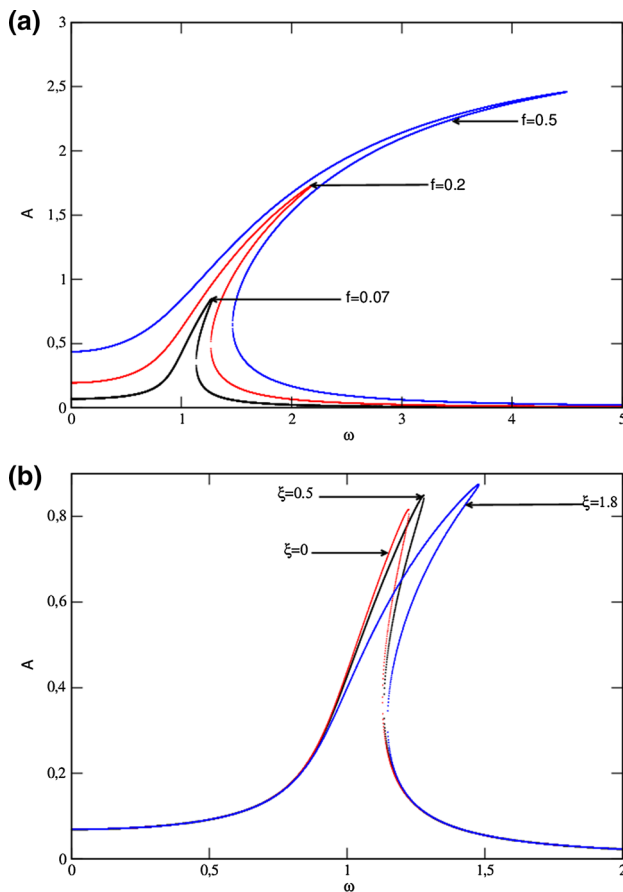
Fig. 2 Effect of the parameters of system on frequency-response curves $A(\omega)$ with $\alpha = 0.07, \beta = 1$: **a** effect of f_0 for $\xi = 0.5$ and **b** effect of ξ for $f_0 = 0.07$

Fig. 3 Effects of the parameters of system on the amplitude-response curves with $\alpha = 0.07, \beta = 1, \omega = 1.25$: **a** $A(\xi)$ for $f_0 = 0.07$ and **b** $A(f_0)$ for $\xi = 0.5$

force (Fig. 3b). From the analysis of these figures, we note that the hysteresis and the amplitude jump phenomena are confirmed and can be controlled and if possible eliminated by the parameters f and ξ. The presence of the phenomenon of hysteresis in the behavior of the amplitude of the oscillations when $\xi \neq 0$, shows that the dependence of the mass as a function of position is a factor favoring the memory effect of the oscillator.

4 Primary resonance

In the case of primary resonant state, the amplitude f of the external excitation is small, that is $f = \epsilon f_0$. The closeness between both natural and external frequencies is given by $\omega = 1 + \epsilon \sigma$, where σ is the detuning parameter. To investigate the resonance states, we use the multiple time scale method [42, 43]. Generally, for analytical investigations, the multiple scales method is used because many types of oscillations can be found in a forced system in addition to harmonic oscillatory states. Such oscillations occur when the
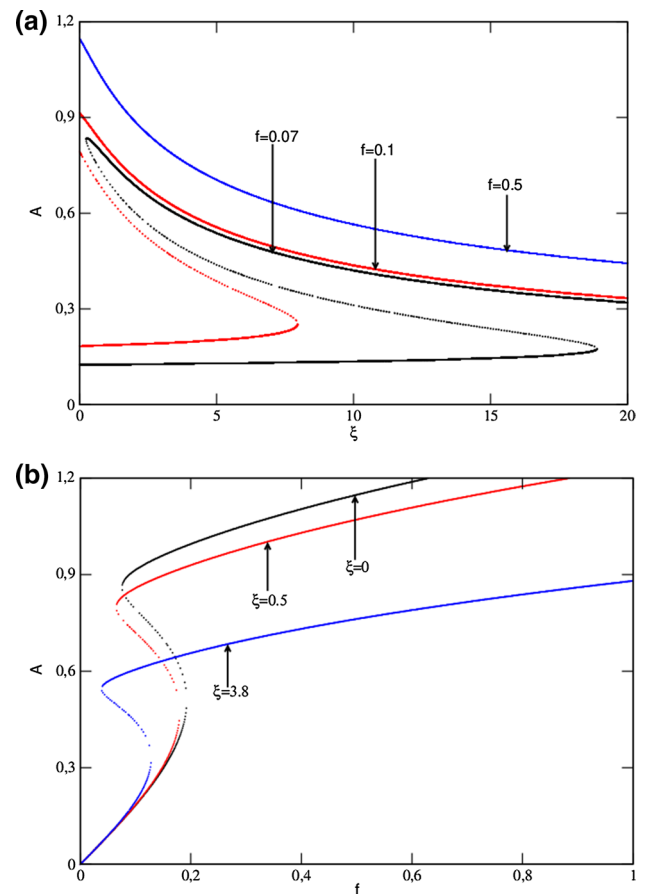
external frequency is too close or too far from the internal frequency, also depending on the external excitation force. Thus, the best tool to use for their investigation is the method of multiple timescales because these oscillations rise at different timescales. For this, we pertube Eq. (3) and we reunite its as:

$$\ddot{x} + x + \epsilon\alpha_0\dot{x} + \epsilon\mu_0 x^2\dot{x} - \epsilon\xi_0 x\dot{x}^2 + \epsilon\kappa_0 x^3\dot{x}^2 + \epsilon\gamma_0 x^3 + \epsilon\lambda_0 x^5 = (1 + \epsilon\eta_0 x^2)\epsilon f_0 \cos\omega t, \tag{7}$$

where

$$\alpha = \epsilon\alpha_0, \mu = \epsilon\mu_0, \xi = \epsilon\xi_0, \kappa = \epsilon\kappa_0,$$
$$\gamma = \epsilon\gamma_0, \lambda = \epsilon\lambda_0, \eta = \epsilon\eta_0.$$

The approximate solution is generally sought as follows:

$$x(\epsilon, t) = x_0(T_0, T_1) + \epsilon x_1(T_0, T_1) + \cdots \tag{8}$$

The first and second times derivatives are defined as follow:

$$\frac{d}{dt} = D_0 + \epsilon D_1 + \cdots, \tag{9}$$

$$\frac{d^2}{dt^2} = D_0^2 + 2\epsilon D_1 D_0 + \cdots, \tag{10}$$

where $D_n^m = \frac{\partial^m}{\partial T_n^m}$ and $T_n = \epsilon^n t$.

Inserting Eqs. (8)—(10) into Eq. (7), we obtain the follow primary resonance amplitude equation (see details in Appendix A)

$$\sigma = \frac{1}{8}(\xi_0 - 3\gamma_0)a^2 - \frac{10}{32}a^4$$
$$\pm \sqrt{\frac{f_0^2}{4a^2} - \left(\frac{1}{2}\alpha_0 + \frac{1}{8}\mu_0 a^2 + \frac{1}{16}\kappa_0 a^4\right)^2}. \tag{11}$$

The stable vibration amplitudes are obtained by applying the Routh–Hurwitz criterion [44, 45] to the following characteristic equation

$$\Lambda^2 + 2T\Lambda + D = 0, \tag{12}$$

where Λ is the eigenvalue of the Jacobian matrix of the linearized system; $T = -\frac{1}{2}(J_{11} + J_{22})$ and $D = J_{11}J_{22} - J_{21}J_{12}$. For the equilibrium point (a_0, Φ_0) to be stable, the Routh–Hurwitz conditions [44, 45] are reduced to the inequalities $T > 0$ and $D > 0$. From Eq. (11), the vibration amplitude of the system is studied as a function of the frequency and the results obtained are plotted in Fig. 4. From this figure, we note the effects of f (Fig. 4a) and of ξ (Fig. 4b) on the primary resonance curve. From the analysis of these figures, it appears that increasing the amplitude f of the external force increases the amplitude of the resonance and decreases the resonance frequency while the opposite effects are obtained when the parameter ξ increases. We also notice the same effects of these parameters on the amplitude jump phenomenon and the domain of unstable vibration amplitudes. In short, the parameter ξ disadvantages these different phenomena while the amplitude of external excitation f favors them.

5 Secondary resonances

The objective of this part of the work is to search superharmonic and subharmonic resonances. Indeed, superharmonic and subharmonic resonances appear for a nonlinear oscillator when the natural frequency ω_0 of this oscillator is a multiple or a submultiple of the frequency ω of the forcing excitation respectively. In other words, there is superharmonic resonance if $n\omega$ is close to the natural frequency of the oscillator and conversely, there is subharmonic resonance if ω is
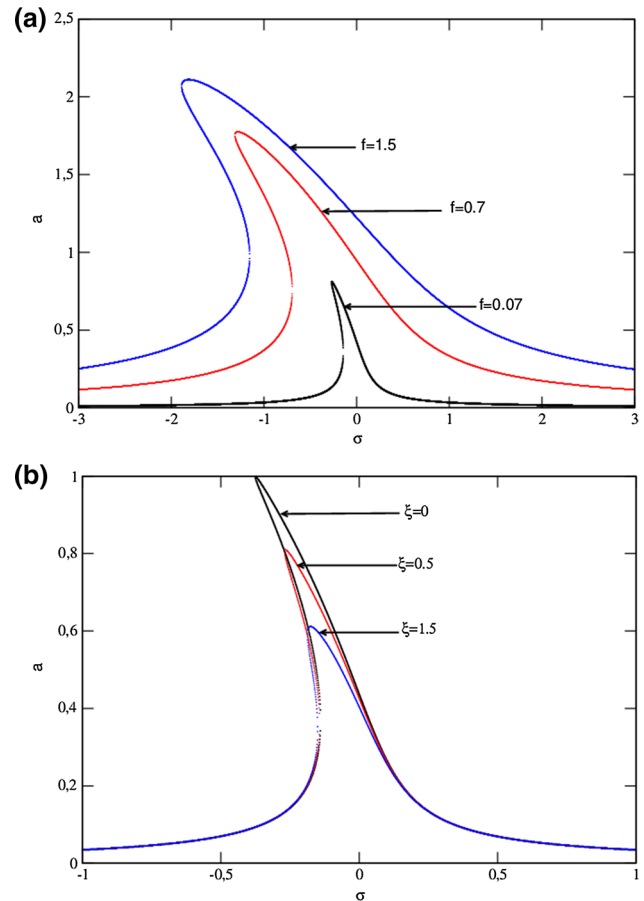

Fig. 4 Effect of the parameters of system on frequency-response curves in primary resonance state with $\alpha = 0.07$, $\beta = 1$: **a** effect of f_0 for $\xi = 0.5$ and **b** effect of ξ for $f0 = 0.07$

close to $n\omega_0$ with n a natural integer. In all the work, $\omega_0 = 1$. In this part, we consider that f is in the order of $\epsilon^0 f$. Then,

$$\ddot{x} + x + \epsilon\alpha_0\dot{x} + \epsilon\mu_0 x^2\dot{x} - \epsilon\xi_0 x\dot{x}^2 + \epsilon\kappa_0 x^3\dot{x}^2$$
$$+ \epsilon\gamma_0 x^3 + \epsilon\lambda_0 x^5 = (1 + \epsilon\eta_0 x^2)f\cos\omega t. \tag{13}$$

By inserting Eqs. (8)–(10) in Eq. (13) we have at:
ϵ^0

$$D_0^2 x_0 + x_0 = f\cos\omega t, \tag{14}$$

and
ϵ^1

$$D_0^2 x_1 + x_1$$
$$= -2D_1 D_0 x_0 - \alpha_0 D_0 x_0 - \mu_0 x_0^2 D_0 x_0 + \xi_0 x_0 (D_0 x_0)^2 \quad (15)$$
$$- \kappa_0 x_0^3 (D_0 x_0)^2 - \gamma_0 x_0^3 - \lambda_0 x_0^5 + \eta_0 f x_0^2 \cos\omega t.$$

The solution of Eq. (14) is

$$x_0 = Ae^{jT_0} + Be^{j\omega T_0} + cc, \tag{16}$$

where $B = \frac{f}{2(1-\omega^2)}$, with $\omega \neq 1$.

Equation (16) in Eq. (15) gives,

$$
\begin{aligned}
D_0^2 x_1 + x_1 = & \left[-2jA' - \alpha_0 jA - \mu_0(jA^2\bar{A} + 2jAB^2) + \right. \\
& + \zeta_0(A^2\bar{A} + 2\omega^2 AB^2) - \kappa_0(2A^3\bar{A}^2 + 6A^2\bar{A}B^2 \\
& + 6\omega^2 A^2\bar{A}B^2 + 6\omega^2 AB^4) - \gamma_0(3A^2\bar{A} + 6AB^2) \\
& \left. - \lambda_0(10A^3\bar{A}^2 + 50A^2\bar{A}B^2 + 30AB^4) + \eta_0 fAB\right]e^{jT_0} \\
& + \left[-j\omega\mu_0 B^3 - \zeta_0\omega^2 B^3 - \gamma_0 B^3 + \frac{1}{2}\eta_0 fB^2 - \kappa_0(2A\bar{A}B^3 \right. \\
& \left. - 6\omega^2 A\bar{A}B^3 - \omega^2 B^5) + \lambda_0(20A\bar{A}B^3 + 5B^5)\right]e^{3j\omega T_0} \\
& + \left[+j\mu_0\bar{A}^2 B + \zeta_0(2\omega\bar{A}^2 B - \bar{A}^2 B) \right. \\
& - \kappa_0(4A\bar{A}^3 B + 6\omega\bar{A}^2 B^3 + 6A\bar{A}^3 B + 3\omega^2\bar{A}^2 B^3) \\
& - 3\gamma_0\bar{A}^2 B - \lambda_0(20A\bar{A}^3 B + 30\bar{A}^2 B^3) \\
& \left. + \frac{1}{2}\eta_0 f\bar{A}^2\right]e^{j(\omega-2)} + + \left[-\kappa_0(2\omega\bar{A}^4 B - 3\bar{A}^4 B) \right. \\
& \left. - 5\lambda_0\bar{A}^4 B\right]e^{j(\omega-4)} + (\kappa_0\omega^2 - \lambda_0)B^5 e^{5j\omega T_0} \\
& + \text{c.c.} + \text{NST.}
\end{aligned}
$$

(17)

From the analysis of (17), it emerges that the oscillator has the possibility of entering into four secondary resonances including two superharmonics $3\omega = 1 + \epsilon\sigma$; $5\omega = 1 + \epsilon\sigma$ and two subharmonics $\omega = 3 + \epsilon\sigma$; $\omega = 5 + \epsilon\sigma$.

5.1 5th order superharmonic resonance

The 5th order superharmonic resonance occurs in the system, when $5\omega = 1 + \epsilon\sigma$. Under this condition, the vibration amplitudes for the 5th order superharmonic resonance verify (see Appendix B):

$$
\begin{aligned}
\sigma = & -\xi_0\left(\frac{1}{8}a^2 + \omega^2 B^2\right) + \gamma_0\left(\frac{3}{8}a^2 + 3B^2\right) \\
& + \kappa_0\left(\frac{1}{16}a^4 + \frac{3}{4}a^2 B^2 + \frac{3}{4}\omega^2 a^2 B^2 + 3\omega^2 B^4\right) \\
& + \lambda_0\left(\frac{5}{16}a^4 - \frac{25}{4}a^2 B^2 + 15B^4\right) - \frac{1}{2}\eta_0 fB \\
& \pm \sqrt{(\kappa_0\omega^2 - \lambda_0)^2\frac{B^{10}}{a^2} - \left[\frac{1}{2}\alpha_0 + \mu_0\left(\frac{1}{8}a^2 + B^2\right)\right]^2}.
\end{aligned}
$$

(18)

The stable vibration amplitudes are obtained by applying the Routh–Hurwitz criterion [44, 45] to the following characteristic equation

$$\Lambda^2 + 2T_1\Lambda + D_1 = 0,$$

(19)

with Λ is the eigenvalue of the Jacobian matrix of the linearized system; $T_1 = -\frac{1}{2}(M_{11} + M_{22})$ and $D_1 = M_{11}M_{22} - M_{21}M_{12}$. By applying the Routh–Hurwitz criterion [44, 45], the amplitudes are stable if and only if $T_1 > 0$ and $D_1 > 0$.

Figure 5 shows the effects of the amplitude of the external excitation (see Fig. 5a) and of the parameter ξ (see Fig. 5b)

on the superharmonic resonance of order 5 whose equation is (18). From Fig. 5a, b, we note that the resonance amplitude and the resonance frequency increase with the parameters f and ξ.

5.2 3rd order superharmonic resonance

The PDM enters superharmonic resonance of order 3 if and only if $3\omega = 1 + \epsilon\sigma$. Under this condition the equation giving the behavior of the vibration amplitudes at this resonance is (see Appendix B):

$$
\begin{aligned}
\sigma = & -\xi_0\left(\frac{1}{8}a^2 + \omega^2 B^2\right) \\
& + \kappa_0\left(\frac{1}{16}a^4 + \frac{3}{4}a^2 B^2 + 3\omega^2 aB^4\right) + \gamma_0\left(\frac{3}{8}a^2 + 3aB^2\right) \\
& + \lambda_0\left(\frac{5}{16}a^4 - \frac{25}{4}a^3 B^2 + 15aB^4\right) - \frac{1}{2}\eta_0 fBa \\
& + \pm\frac{1}{a}\sqrt{\mu_0^2\omega^2 B^6 + Q_s},
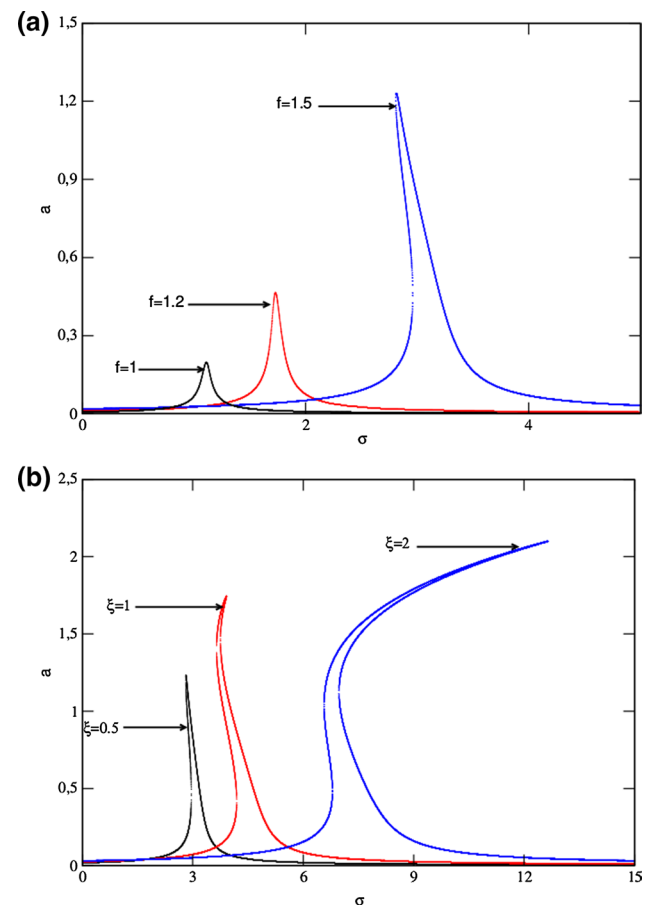\end{aligned}
$$

(20)

Fig. 5 Effect of the parameters of system on frequency-response curves in order 5 superharmonic resonance with $\alpha = 0.07, \beta = 1$: **a** effect of f for $\xi = 0.5$ and **b** effect of ξ for $f = 1.5$

with

$$Q_s = \left[-\xi_0 \omega^2 B^3 - \gamma_0 B + \frac{1}{2}\eta_0 f B^2 \right.$$
$$\left. -\kappa_0 \left(\frac{1}{2} a^2 B^3 - \frac{3}{2}\omega^2 B^3 - \omega^2 B^5 \right) \right.$$
$$\left. -\lambda_0 \left(5a^2 B^3 + 5B^5 \right) \right]^2 - \left[-\frac{1}{2}\alpha_0 a - \mu_0 \left(\frac{1}{8}a^3 + aB^2 \right) \right]^2.$$

The characteristic equation giving the stable amplitudes is

$$\Lambda^2 + 2T_2\Lambda + D_2 = 0, \qquad (21)$$

with Λ is the eigenvalue of the Jacobian matrix of the linearized system; $T_2 = -\frac{1}{2}(N_{11} + N_{22})$ et $N_2 = N_{11}N_{22} - N_{21}N_{12}$. By virtue of the Routh–Hurwitz criterion [44, 45], the amplitudes of the oscillations at the third-order superharmonic resonance are stable if and only if $T_2 > 0$ and $D_2 > 0$.

Equation (20) represents the relation which gives the amplitude of the vibrations of the system at order 3 superharmonic resonance in function of the frequency as well as all of the oscillator parameters. The evolution of this amplitude as a function of the frequency, of f and of ξ is plotted in Fig. 6a, b respectively. Note that f and ξ also increase the amplitude and the resonance frequency as well as the domain of unstable amplitudes.

5.3 5th order subharmonic resonance

Here, $\omega = 5 + \epsilon\sigma$. With this condition the evolution of the vibration amplitudes as a function of the parameters of the system is given by (see Appendix C):

$$\sigma = -5\xi_0 \left(\frac{1}{8}a^2 + B^2 \right)$$
$$+ 5\kappa_0 \left(\frac{1}{16}a^4 + \frac{3}{4}a^2 B^2 + \frac{3}{4}\omega^2 a^2 B^2 + 3\omega^2 B^4 \right)$$
$$+ 5\gamma_0 \left(\frac{3}{8}a^2 + 3B^2 \right)$$
$$+ 5\lambda_0 \left(\frac{5}{16}a^4 - \frac{25}{4}a^2 B^2 + 15B^4 \right) - \frac{5}{2}\eta_0 f B + \pm 5$$
$$\times \sqrt{\frac{1}{256} \left[\kappa_0(2\omega - 3) + 5\lambda_0 \right]^2 B^2 a^6 - \left[\frac{1}{2}\alpha_0 + \mu_0 \left(\frac{1}{8}a^2 + B^2 \right) \right]^2}. \qquad (22)$$

The stable and unstable amplitudes are obtained from the following characteristic equation:

$$\Lambda^2 + 2T_3\Lambda + D_3 = 0, \qquad (23)$$

with Λ is the eigenvalue of the Jacobian matrix of the linearized system; $T_3 = -\frac{1}{2}(P_{11} + P_{22})$ and $D_3 = P_{11}P_{22} - P_{12}P_{21}$. The oscillations are stable if and only if $T_3 > 0$ and $D_3 > 0$.

Figure 7 shows the effects of the parameters f (Fig. 7a) and ξ (Fig. 7b) on order 5 subharmonic resonance. It
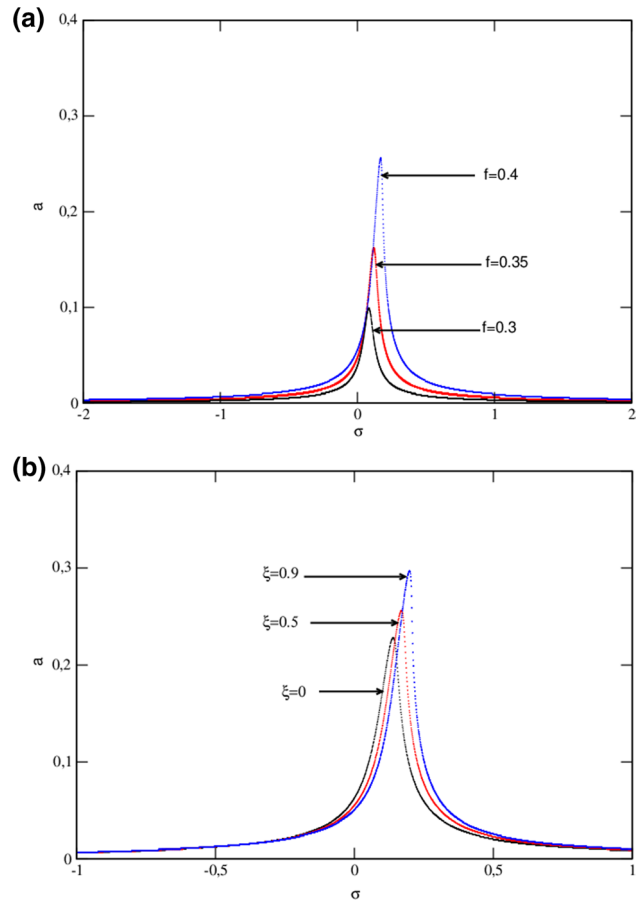

Fig. 6 Effect of the parameters of system on frequency-response curves in order 3 superharmonic resonance with $\alpha = 0.07, \beta = 1$: **a** effect of f for $\xi = 0.5$ and **b** effect of ξ for $f = 0.4$

emerges from the analysis of this figure that order 5 subharmonic resonance increases with the increase of f or of ξ.

5.4 3rd order subharmonic resonance

This resonance takes place when $\omega = 3 + \epsilon\sigma$. Under this condition, when we cancel the secular terms, we obtain after simplification (see details in Appendix C):

$$\sigma = -3\xi_0 \left(\frac{1}{8}a^2 + \omega^2 B^2 \right) + 3\gamma_0 \left(\frac{3}{8}a^2 + 3B^2 \right)$$
$$+ 3\lambda_0 \left(\frac{5}{16}a^4 - \frac{25}{4}a^2 B^2 + 15B^4 \right)$$
$$+ 3\kappa_0 \left(\frac{1}{16}a^4 + \frac{3}{4}a^2 B^2 + \frac{3}{4}\omega^2 a^2 B^2 + 3\omega^2 B^4 \right)$$
$$- \frac{3}{2}\eta_0 f B + \pm \frac{3}{a}\sqrt{\frac{1}{16}\mu_0^2 a^4 B^2 + Q_r}, \qquad (24)$$
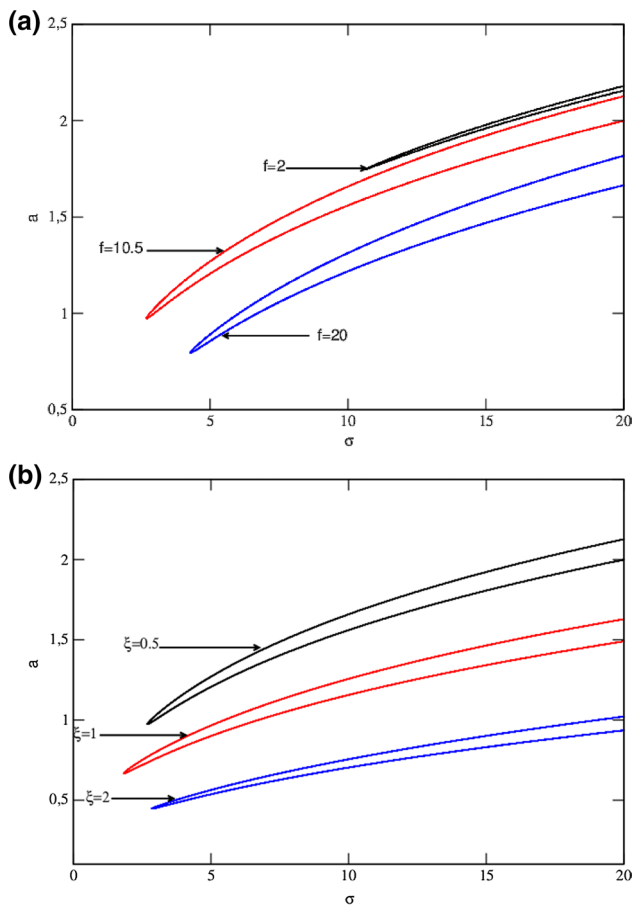
where

(a)

(b)

Fig. 7 Effect of the parameters of system on frequency-response curves in order 5 subharmonic resonance with $\alpha = 0.07, \beta = 1$: **a** effect of f for $\xi = 0.5$ and **b** effect of ξ for $f = 10.5$
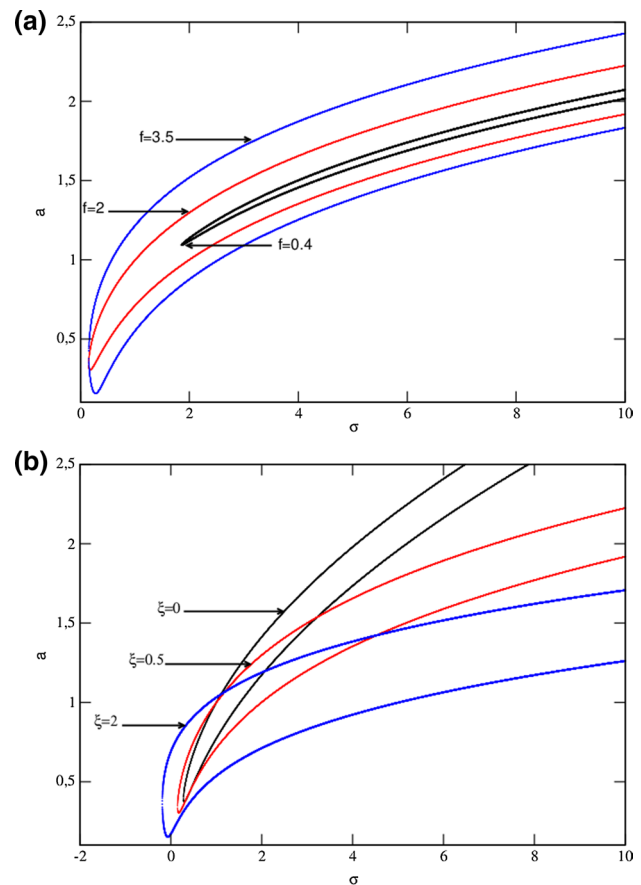
(a)

(b)

Fig. 8 Effect of the parameters of system on frequency-response curves in order 3 subharmonic resonance with $\alpha = 0.07, \beta = 1$: **a** effect of f for $\xi = 0.5$ and **b** effect of ξ for $f = 2$

$$Q_r = \left[\xi_0\left(\frac{1}{2}\omega a^2 B - \frac{1}{4}a^2 B\right)\right.$$
$$- \kappa_0\left(\frac{1}{4}a^4 B + \frac{3}{2}\omega a^2 B^3 + \frac{3}{8}a^4 B + \frac{3}{4}\omega^2 a^2 B^3\right)$$
$$\left.- \lambda_0\left(\frac{5}{4}a^4 B + \frac{15}{2}a^2 B^3\right) - \frac{3}{4}\gamma_0 a^2 B + \frac{1}{8}\eta_0 f a^2\right]^2$$
$$- \left[-\frac{1}{2}\alpha_0 a - \mu_0\left(\frac{1}{8}a^3 + aB^2\right)\right]^2.$$

The stable vibration amplitudes are obtained by applying the Routh–Hurwitz criterion [44, 45] to the following characteristic equation

$$\Lambda^2 + 2T_4\Lambda + D_4 = 0, \tag{25}$$

with Λ is the eigenvalue of the Jacobian matrix of the linearized system; $T_4 = -\frac{1}{2}(Q_{11} + Q_{22})$ and $D_4 = (Q_{11}Q_{22} - Q_{12}Q_{21})$.

The amplitudes of oscillations for order 3 subharmonic resonance are stable if and only if $T_4 > 0$ and $D_4 > 0$.

Equation (24) represents the relation which gives the amplitude of the vibrations of the system at order 3

subharmonic resonance in function of the frequency as well as all of the oscillator parameters. The evolution of this amplitude as a function of the frequency, of f and of ξ is plotted in Fig. 8a, b respectively. We note that f and ξ also have the same effects as in the case of subharmonic resonance of order 5.

6 Dynamic analysis of a position dependent mass-driven Duffing-type oscillator

Coexisting attractors, hysteresis and chaos have been studied in different biological, physical and non-physical systems by using numerical methods [19–23]. Because of their complexity, a position dependent mass-driven Duffing-type oscillator is potential system that can exhibit these complicated behaviors and that's why this section is dedicated to bifurcation, route to chaos and coexistence of attractors. Indeed, using the fourth order Runge–Kutta integration algorithm, we solve numerically Eq. (26) of a position dependent

mass oscillator and bifurcation diagrams, Lyapunov exponents, phase portraits and basin of attraction are plotted with the initial condition ($x = 3, \dot{x} = y = -1$). Equation (26) is

$$\frac{dx}{dt} = y,$$

$$\frac{dy}{dt} = \sqrt{1 + \xi x^2}(-\omega_0^2 x - \beta x^3 - \alpha y) + \frac{\xi x y^2}{1 + \xi x^2} \quad (26)$$

$$+ f\sqrt{1 + \xi x^2} \cos \omega t.$$

First, we looked for the dynamics of the oscillator studied at the primary resonance and at the other resonances by using the base values [6] of the parameters with the amplitude f of the external excitation as the parameter of bifurcation. Thus, for $f \in [0, 30]$, the dynamics of a position dependent mass-driven Duffing-type oscillator is very rich and can be regular or chaotic (see Fig. 9). Indeed, for $\alpha = 0.2, \beta = 1, \xi = 0.5, \omega_0 = 1$ and $\omega = 1$, the oscillator has a regular behavior of period $1T$ if $0 \leq f < 5.34763$ then go to period $3T$ if $5.34763 \leq f < 12.4482$; then the behavior of the oscillator becomes of period $2T$ when $12.4482 \leq f < 13.2618$. Beyond $f = 13.2618$, the oscillator has a dynamic of period $4T$, multiperiodic then becomes chaotic when $17.5148 \leq f < 19.142$ crossing a very small area on which it is almost periodic. When $19.142 \leq f < 21.0651$, the behavior of the oscillator is multi-periodic and then becomes chaotic if $21.0651 \leq 21.5089$, quasi-periodic if $21.5089 \leq 21.6938$, chaotic when $21.6938 \leq f < 22.3225$, multi-periodic for $22.3225 \leq f < 22.6553$, chaotic if $22.6553 \leq f < 24.3565$ and finally regular of period $5T$ when $f \geq 24.3565$. Finally, to characterize the coexistence

of attractors in the system we use the method presented in [34–41]. Thus, we compare the two bifurcation diagrams and their corresponding Lyapunov exponents obtained by increasing f from 0 to 30 (curve in blue) with the bifurcation diagram and the Lyapunov exponent obtained by decreasing f from 30 to 0 (red curve). We note through Fig. 9 we can see that for $\alpha = 0.2, \beta = 1, \xi = 0.5$ a position dependent mass-driven Duffing-type oscillator does not suffer from the phenomenon of coexistence of attractors because the amplitudes of the oscillations and the nature of the dynamics are the same in each of the fields of study. We note through our study that the oscillator has regular behaviors of period $1T$ and $4T$ in the case of the subharmonic resonance of order 5 and has only periodic behavior of period $1T$ in the case of subharmonic resonance of order 3 which figures are not present here. We also notice that in these states of resonance and in the conditions of values of the parameters defined here the system does not undergo the phenomenon of the coexistence of attractors. It appears that the dynamics of a position dependent mass-driven Duffing-type oscillator is very rich in its state of primary resonance than in the cases of subharmonic resonances and superharmonic resonances whose diagrams are not shown here because of the similarity they have with the resonance diagrams subharmonic. Secondly, we studied the position dependent mass-driven Duffing-type oscillator by fixing all other parameters and varying the PDM parameter ξ from 0 to 5. Thus, Fig. 10 obtained for $\alpha = 0.2, \beta = 1, \omega_0 = 0.5, \omega = 1$ and $f = 8.5$ represents the bifurcation diagram (Fig. 10a) and its Lyapunov exponents (Fig. 10b) when ξ increases from 0 to 5 (blue curve) and when ξ decreases of 5 to 0 (red curve). We notice that when

Fig. 9 Bifurcation diagram and corresponding Lyapunov exponent vs the amplitude f in primary resonant state with $\alpha = 0.2, \beta = 1, \xi = 0.5, \omega_0 = 1$ and $\omega = 1$. Bifurcation diagrams and their corresponding Lyapunov exponents are obtained by scanning the parameter f upwards (blue) and downwards (red)
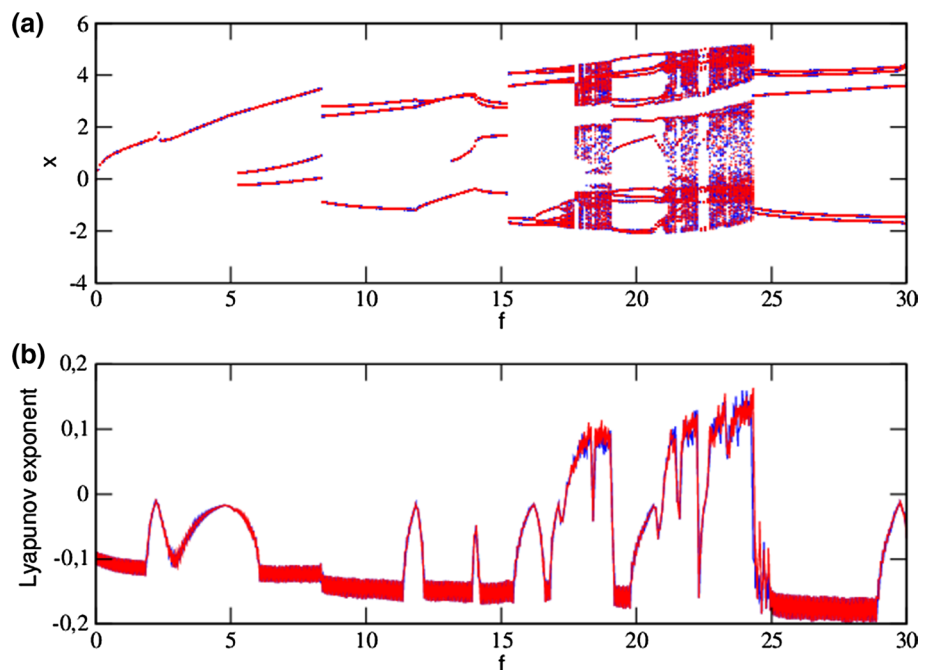
$f = 8.5$ (Fig. 10) or $f = 12.6$ (Fig. 11), the coexistence of attractors appear for the PDM oscillator. In fact, we observe through Figs. 10 and 11 only when the PDM parameter ξ varies from 0 to 5, and from then from 5 to 0 the oscillations of the PDM oscillator do not follow the same path on both sides because do not have by the same amplitudes and do not have the same natures. This remark justifies that the PDM oscillator undergoes a phenomenon of multistability. More precisely, there appear areas in which multi-period attractors coexist, domains in which chaotic attractors coexist and domains for which multi-periodic attractors coexist.

It appears that in these different domains where this complex phenomenon occur, it would be very difficult to say with certainty the nature of the behaviors and also the amplitude of vibration of this oscillator thus justifying the complexity of the PDM system and the great sensitivity to the initial conditions of the latter. To illustrate this sensitivity to the initial conditions and the coexistence of various attractors, we have drawn the basin of attraction (Fig. 12) and the phase portraits (Figs. 13 and 14). Figure 12 shows that all initial conditions (x_0, y_0) chosen in the blue domain give a chaotic dynamic while in the white part we get a regular behavior.

Fig. 10 Bifurcation diagram and corresponding Lyapunov exponent vs ξ with $\alpha = 0.2, \beta = 1, \omega_0 = 0.5, \omega = 1$ and $f = 8.5$. Bifurcation diagrams and their corresponding Lyapunov exponents are obtained by scanning the parameter ξ upwards (blue) and downwards (red)
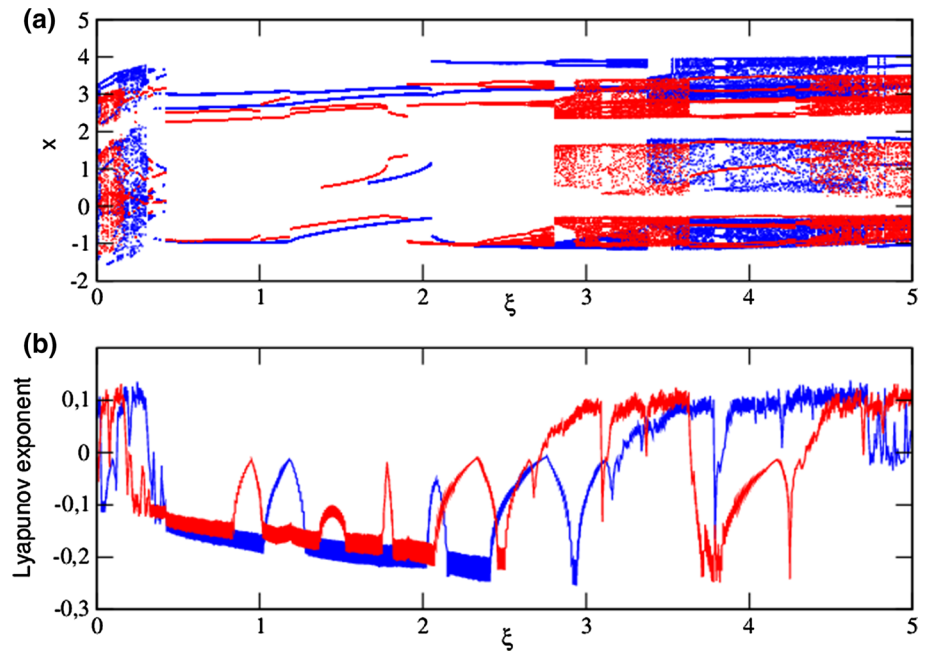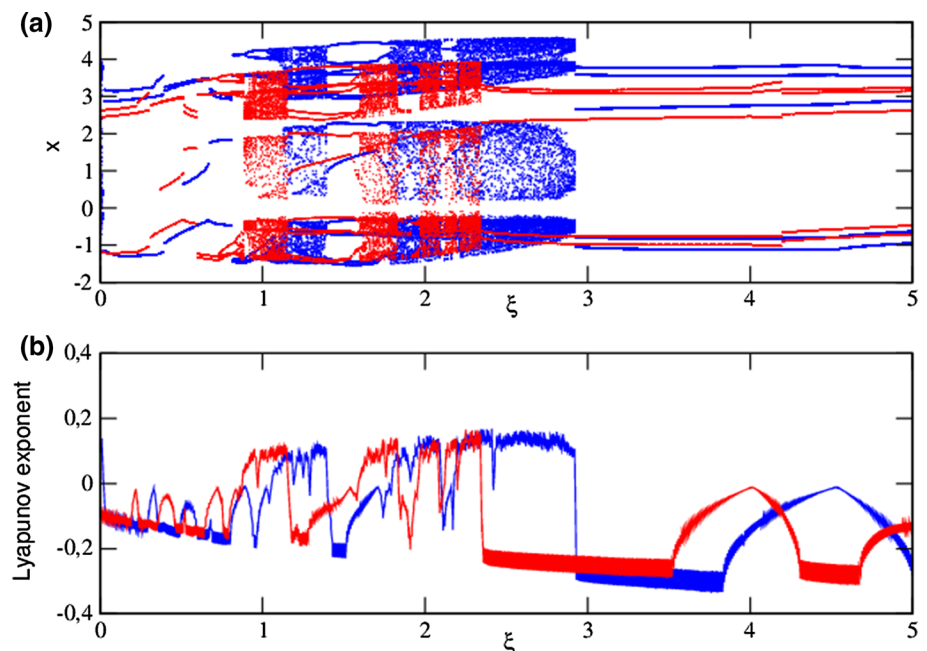

Fig. 11 Bifurcation diagram and corresponding Lyapunov exponent vs ξ with parameters of Fig. 10 and $f = 12.6$. Bifurcation diagrams and their corresponding Lyapunov exponents are obtained by scanning the parameter ξ upwards (blue) and downwards (red)
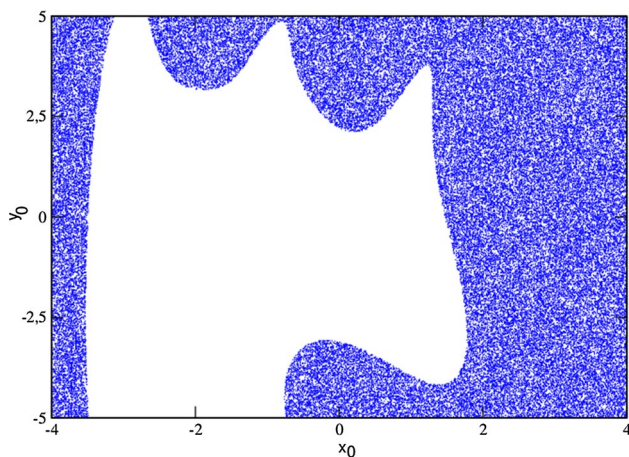
Fig. 12 Basin of attraction of a position dependent mass-driven Duffing-type oscillator with $\xi = 0.25$ and other parameters of Fig. 10. The values of the initial conditions selected in blue regions lead to chaotic behavior while the white regions correspond, to periodic behavior

This is confirmed by the phase portraits of Fig. 13 where the phase portrait in blue color obtained for $(x_0 = 3, y_0 = -1)$ is chaotic while the phase portrait in red color corresponding $(x_0 = 0.5, y_0 = 0.5)$ is periodic. Finally, Fig. 14 shows the coexistence of the variousattractors predicted by the bifurcation diagram and the Lyapunov exponent of Fig. 11 with appropriate values of the PDM parameter ξ.

7 Conclusions

In this work, it was studied the complex nonlinear dynamics of a position dependent mass-driven Duffing-type oscillator (PDM oscillator). Initially, we considered the approximate equation of the PDM oscillator to find its harmonic oscillations by the harmonic balance method then its states of primary, superharmonic and subharmonic resonances by the multiple scale method. It is obtained domains of stable and unstable amplitudes, amplitude jump and hysteresis phenomena which strongly depend on the PDM parameter ξ, the amplitude and the frequency of the external excitation force. A comparison of the analytical results resulting from the treatment of the approximate equation was made with the numerical results using the approximate and exact equations of the PDM oscillator. From this comparison, it emerges that these different results are in very good agreement thus validating the approximate model and the techniques used. Secondly, we used the bifurcation diagram, the Lyapunov exponents, the basin of attraction and the phase portraits to explore the different dynamics of the PDM oscillator. It emerges from these studies that the PDM oscillator has a very rich dynamic for α, β fixed and f, ξ variables in the case of primary resonance and has only regular behaviors in the case of secondary resonances. Thus in its primary
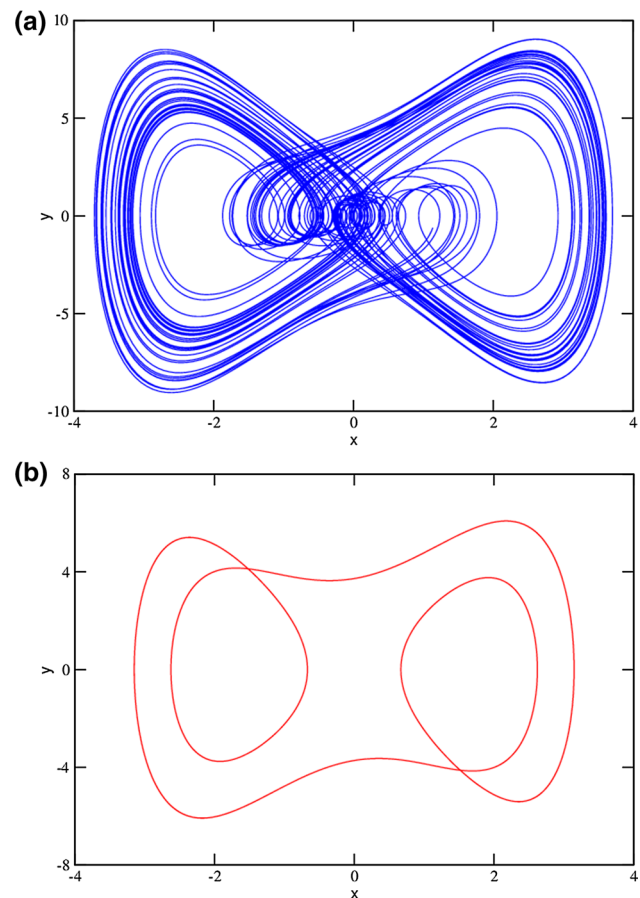

Fig. 13 Coexistence of chaotic attractor and periodic attractor of a position dependent mass-driven Duffing-type oscillator with parameters of Fig. 10 and $\xi = 0.25$: **a** Chaotic attractor (blue color) for initial condition $(3, -1)$ and periodic attractor (red color) for initial condition, **b** $(0.5, 0.5)$

resonance state, the PDM system can have periodic, multi-periodic, quasi-periodic and chaotic behaviors. Moreover, the analysis of the coexistence of attractors reveals that when ξ is fixed and that f is the bifurcation parameter the PDM oscillator does not follow any of this complex phenomenon. On the other hand, for outside of its resonance states, when the PDM parameter is varied in precise domains, it occurs for well-fixed values of the amplitude of the excitation force, the phenomenon of coexistence of various attractors for the system studied. These different results prove that the most important parameters to predict and control the different dynamics and complex phenomena of the PDM oscillator are the external excitation force and the PDM parameter ξ. It results from it a complexity of the dynamics of the oscillator due to the internal influence between f and ξ. The essential distinction between the constant mass and the variable mass case rests in the fact that the presence of the parameter ξ not only enhances the rapidity of such transitions but also initiates complicated nature of dynamics of the system. Finally,
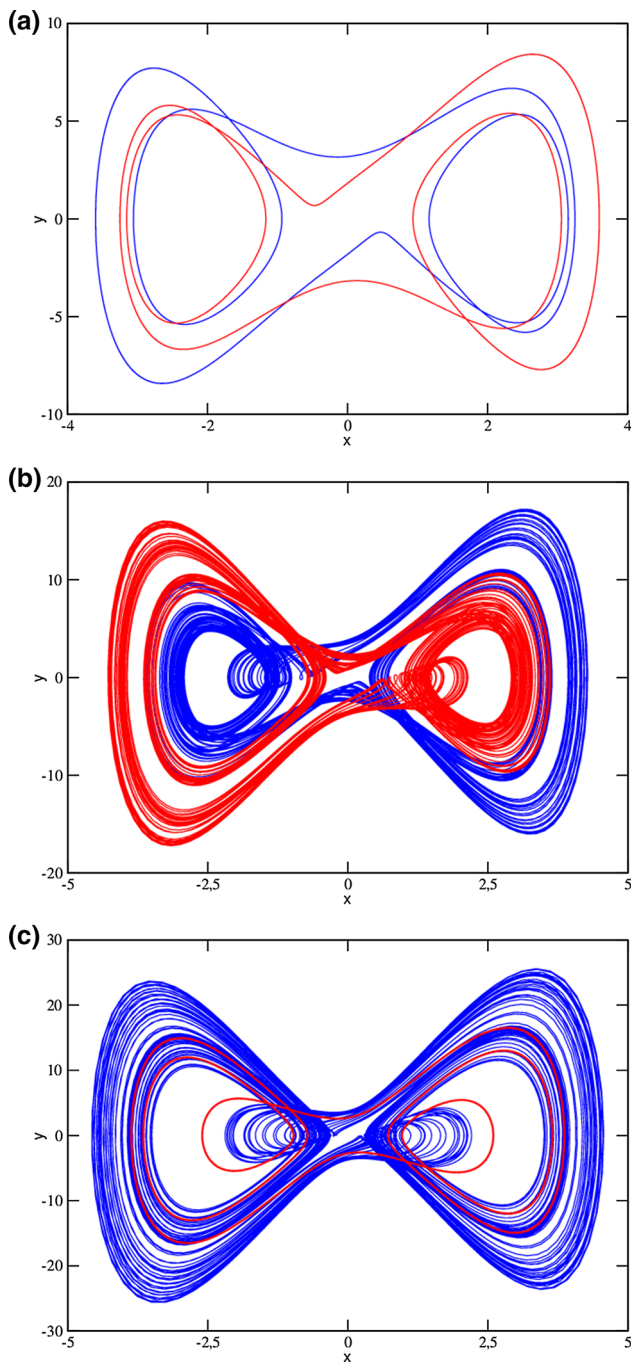
(a)

(b)

(c)

Fig. 14 Various phase spaces of a position dependent mass-driven Duffing-type oscillator with parameters of Fig. 11 for: **a** $\xi = 0.4$ and initial conditions, blue color $(3, -1)$ and red color $(0, 0)$ showing coexisting of two $3T$−periodic attractors; **b** $\xi = 1.1$ and initial conditions, blue color $(3, -1)$ and red color $(4, 3)$ showing coexisting of two chaotic attractors; **c** $\xi = 2.7$ and initial conditions, blue color $(3, -1)$ (chaotic attractor) and red color $(4, 3)$ (multi-periodic attractor)

the coexistence of attractors in the PDM can help reduce its performance. It is for this reason that we consider controlling this complex phenomenon in our future work on PDM. Also,the appearance of horseshoes chaos is major them in

nonlinear sciences researches. It is thus important to analyse the horseshoes chaos and its control in PDM system and evaluate the effect of the PDM coefficient in appearance or disappearance of this chaos in our future work on PDM.

Appendix A : Primary resonance

Inserting Eqs. (8)–(10) into Eq. (7), and after some algebraic manipulations, we obtain at: ϵ^0

$$D_0^2 x_0 + x_0 = 0 \tag{27}$$

and
$$\epsilon^1$$

$$
\begin{aligned}
D_0^2 x_1 + x_1 = &-2D_1 D_0 x_0 - \alpha_0 D_0 x_0 - \mu_0 x_0^2 D_0 x_0 \\
&+ \xi_0 x_0 (D_0 x_0)^2 - \kappa_0 x_0^3 (D_0 x_0)^2 - \gamma_0 x_0^3 - \lambda_0 x_0^5 \\
&+ f_0 \cos \omega t.
\end{aligned}
\tag{28}
$$

The general solution of Eq. (27), is:

$$x_0 = A(T_1)e^{jT_0} + \text{cc}, \tag{29}$$

where "cc" designate the conjugate complex themes. Inserting Eq. (29) into Eq. (28), we have:

$$
\begin{aligned}
&D_0^2 x_1 + x_1 \\
&= \Big[-2jA' - j\alpha_0 A - j\mu_0 A^2\bar{A} + \xi_0 A^2\bar{A} - 2j\kappa_0 A^3\bar{A}^2 \\
&\quad -3\gamma_0 A^2\bar{A} - 10\lambda_0 A^3\bar{A}^2 + \frac{f_0}{2}e^{j\sigma T_1} \Big] e^{jT_0} + \text{cc} + \text{NST},
\end{aligned}
\tag{30}
$$

where NST denotes the terms does not produce secular terms. Now, we introduce the amplitude $A(T_1)$ given by the following polar form:

$$A(T_1) = \frac{1}{2}a(T_1)e^{j\theta(T_1)}, \tag{31}$$

and eliminate the secular themes of Eq. (30). Separating real and imaginary parts, we obtain the following modulation equations:

$$D_1 a = -\frac{1}{2}\alpha_0 a - \frac{1}{8}\mu_0 a^3 - \frac{1}{16}\kappa_0 a^5 + \frac{f_0}{2}\sin\varPhi, \tag{32}$$

$$aD_1\theta = -\frac{1}{8}\xi_0 a^3 + \frac{3}{8}\gamma_0 a^3 + \frac{10}{32}\lambda_0 a^5 - \frac{f_0}{2}\cos\varPhi, \tag{33}$$

with $\varPhi = \sigma T_1 - \theta$. By looking for the equilibrium state solutions, we obtain after some algebraic manipulations Eq. (11).

Now, we analyze the stability of the non-trivial fixed points of the modulation equations (32) and (33). For this end, we let:

$$a = a_0 + a_1, \Phi = \Phi_0 + \Phi_1, \tag{34}$$

where a_0 and Φ_0 are the non-trivial solutions of stable equilibrium states and a_1 and Φ_1 are infinitesimal perturbations. Substituting (34) into (32) and (33), and then canceling nonlinear terms enables us to obtain:

$$D_1 a_1 = J_{11} a_1 + J_{12} \Phi_1, \tag{35}$$

$$D_1 \Phi_1 = J_{21} a_1 + J_{22} \Phi_1 \tag{36}$$

with

$$J_{11} = -\frac{1}{2}\alpha_0 - \frac{3}{8}\mu_0 a_0^2 - \frac{5}{16}\kappa_0 a_0^4, \tag{37}$$

$$J_{12} = -\sigma_0 a_0 + \frac{1}{8}(3\gamma_0 - \xi_0)a_0^3 + \frac{10}{32}\lambda_0 a_0^5, \tag{38}$$

$$J_{21} = -\frac{3}{8}(\xi_0 - 3\gamma_0)a_0 - \frac{46}{32}\lambda_0 a_0^3 + \frac{\sigma_0}{a_0}, \tag{39}$$

$$J_{22} = -\frac{1}{2}\alpha_0 - \frac{1}{8}\mu_0 a_0^2 - \frac{1}{16}\kappa_0 a_0^5. \tag{40}$$

We obtain the following characteristic equation (12).

Appendix B: Superharmonic resonances

So by using the condition $5\omega = 1 + \epsilon\sigma$ and by canceling the resonant terms in this case for (17), we find after some transformations

$$D_1 a = -\frac{1}{2}\alpha_0 a - \mu_0\left(\frac{1}{8}a^3 + aB^2\right) \\ + (\kappa_0\omega^2 - \lambda_0)B^5 \sin\Phi, \tag{41}$$

and

$$aD_1\Phi = a\sigma + \xi_0\left(\frac{1}{8}a^3 + \omega^2 aB\right) \\ - \kappa_0\left(\frac{1}{16}a^5 + \frac{3}{4}a^3B^2 + \frac{3}{4}\omega^2 a^3B^2 + 3\omega^2 aB^4\right) \\ - \gamma_0\left(\frac{3}{8}a^3 + aB^2\right) - \lambda_0\left(\frac{5}{16}a^5 - \frac{25}{4}a^3B^2 + 15aB^4\right) \\ + \frac{1}{2}\eta_0 faB + (\kappa_0\omega^2 - \lambda_0)B^5 \cos\Phi, \tag{42}$$

with $\Phi = \sigma T_1 - \theta$. Taking the stable equilibrium solutions and after simplification, the equation verified by the resonance amplitude of order 5 is given by Eq. (18). The phase Φ for the superharmonic resonance of order 5 is given by

$$\Phi = \arctan\left(-\frac{S_{01}}{S_{02}}\right), \tag{43}$$

with

$$S_{01} = \frac{1}{2}\alpha_0 a_0 + \mu_0\left(\frac{1}{8}a_0^3 + a_0B^2\right) \tag{44}$$

and

$$S_{02} = a_0\sigma + \xi_0\left(\frac{1}{8}a_0^3 + \omega^2 a_0B^2\right) \\ - \kappa_0\left(\frac{1}{16}a_0^5 + \frac{3}{4}a_0^3B^2 + 3\omega^2 a_0B^4 \\ + \frac{3}{4}\omega^2 a_0^3B^2\right) - \gamma_0\left(\frac{3}{8}a_0^3 + 3a_0B^2\right) \\ - \lambda_0\left(\frac{5}{16}a_0^5 - \frac{25}{4}a_0^3B^2 + 15a_0B^4\right) + \frac{1}{2}\eta_0 fa_0B.$$

Let us now study the stability of the solutions. So, using the solution (34) and taking the linear form of (41) and (42) around (a_0, Φ_0), we get:

$$\begin{aligned} D_1 a_1 &= M_{11} a_1 + M_{12} \Phi_1, \\ D_1 \Phi_1 &= M_{21} a_1 + M_{22} \Phi_1, \end{aligned} \tag{45}$$

with

$$M_{11} = -\frac{1}{2}\alpha_0 - \mu_0\left(\frac{1}{8}a_0^2 + B^2\right),$$

$$M_{12} = -a_0\sigma + \eta_0\left(\frac{1}{8}a_0^3 + \omega^2 a_0B^2\right) \\ + \kappa_0\left(\frac{1}{16}a_0^5 + \frac{3}{4}a_0^3B^2 + \frac{3}{4}\omega^2 a_0^3B^2 + 3\omega^2 a_0B^4\right) \\ + \gamma_0\left(\frac{3}{8}a_0^3 + 3a_0B^2\right) \\ + \lambda_0\left(\frac{5}{8}a_0^5 - \frac{25}{4}a_0^3B^2 + 15a_0B^4\right) - \frac{1}{2}\eta_0 fa_0B,$$

$$M_{21} = -\frac{1}{4}\eta_0 a_0 - \kappa_0\left(\frac{1}{4}a_0^3 + \frac{3}{2}a_0B^2 + \frac{3}{2}\omega^2 a_0B^2\right) \\ + \lambda_0\left(\frac{5}{4}a_0^3 - \frac{25}{2}a_0B^2\right) + \frac{1}{a_0^2}[a_0\sigma - \eta_0\left(\frac{1}{8}a_0^3 + \omega^2 a_0B\right) \\ - \kappa_0\left(\frac{1}{16}a_0^5 + \frac{3}{4}a_0^3B^2 + 3\omega^2 a_0B^4\right) - \gamma_0\left(\frac{3}{8}a_0^3 + 3a_0B^2\right) \\ - \frac{3}{4}\gamma_0 a_0 - \lambda_0\left(\frac{5}{16}a_0^5 - \frac{25}{4}a_0^3B^2 + 15a_0B^4\right) + \frac{1}{2}\eta_0 fa_0B],$$

$$M_{22} = -\frac{1}{2}\alpha_0 - \mu_0\left(\frac{1}{8}a_0^2 + B^2\right).$$

The characteristic equation of Jacobian is given by Eq. (19)

The second part of this appendix is dedicated to details on the third-order superharmonic resonance. Thus, for the 3rd order superharmonic resonance, $3\omega = 1 + \epsilon\sigma$ By canceling the secular terms in (17), after appropriate algebraic manipulations we have:

$$D_1 a = -\frac{1}{2}\alpha_0 a - \mu_0\left(\frac{1}{8}a^3 + aB^2\right) - \mu_0\omega B^3 \cos\Phi$$
$$+ \left[-\xi_0\omega^2 B^3 - \gamma_0 B^3 + \frac{1}{2}\eta_0 fB^2\right.$$
$$- \kappa_0\left(\frac{1}{2}a^2 B^3 - \frac{3}{2}\omega^2 a^2 B^3 - \omega^2 B^5\right)$$
$$\left.- \lambda_0\left(5a^2 B^3 + 5B^5\right)\right]\sin\Phi, \tag{46}$$

and

$$aD_1\Phi = \sigma a + \xi_0\left(\frac{1}{8}a^3 + \omega^2 aB^2\right)$$
$$- \kappa_0\left(\frac{1}{16}a^5 + \frac{3}{4}a^3 B^2 + 3\omega^2 aB^4\right)$$
$$- \gamma_0\left(\frac{3}{8}a^3 + 3aB^2\right) - \lambda_0\left(\frac{5}{16}a^5 - \frac{25}{4}a^3 B^2 + 15aB^2\right)$$
$$+ \frac{1}{2}\eta_0 faB + \mu_0\omega B^3 \sin\Phi + \left[-\xi_0\omega^2 B^3\right.$$
$$- \gamma_0 B^3 + \frac{1}{2}\eta_0 fB^2$$
$$- \kappa_0\left(\frac{1}{2}a^2 B^3 - \frac{3}{2}\omega^2 a^2 B^3 - \omega^2 B^5\right)$$
$$\left.- \lambda_0\left(5a^2 B^3 + 5B^5\right)\right]\cos\Phi, \tag{47}$$

with $\Phi = \sigma T_1 - \theta$. By looking for the solutions of equilibrium states, we find the equation verified by the amplitudes of the oscillations at order 3 superharmonic resonance and we obtain Eq. (20).

The phase Φ in this case is given by

$$\Phi = \arctan\frac{S_2 S_3 + \mu_0\omega B^3 S_4}{S_1 S_4 - \mu_0\omega B^3 S_2}, \tag{48}$$

where

$$S_1 = -\xi_0\omega^2 B^3 - \gamma_0 B^3 - \lambda_0(5a_0^2 B^3 + 5B^5)$$
$$+ \frac{1}{2}\eta_0 fB^2 - \kappa_0\left(\frac{1}{2}a_0^2 B^3 - \frac{3}{2}\omega^2 a_0^2 B^3 - \omega^2 B^5\right),$$
$$S_2 = \frac{1}{2}\alpha_0 a_0 + \mu_0\left(\frac{1}{8}a_0^3 + a_0 B^2\right),$$
$$S_3 = -\xi_0\omega^2 B^3 - \gamma_0 B^3 - \lambda_0(5a_0^2 B^5 + 5B^5)$$
$$+ \frac{1}{2}\eta_0 fB^2 - \kappa_0\left(\frac{1}{2}a_0^2 B^3 - \frac{3}{2}\omega^2 a_0^2 B^3 - \omega^2 B^5\right),$$
$$S_4 = -a_0\sigma - \eta_0\left(\frac{1}{8}a_0^3 + \omega^2 a_0 B^2\right)$$
$$+ \kappa_0\left(\frac{1}{16}a_0^5 + \frac{3}{4}a_0^3 B^2 + 3\omega^2 a_0 B^4\right)$$
$$+ \gamma_0\left(\frac{3}{8}a_0^3 + 3a_0 B^2\right) - \frac{1}{2}\eta_0 fBa_0$$
$$+ \lambda_0\left(\frac{5}{16}a_0^5 - \frac{25}{4}a_0^3 B^2 + 15a_0 B^4\right).$$

Now, let us go to the study of the stability of the amplitudes of the oscillations using the solution (34). Taking the linear form of (46) and (47) around (a_0, Φ_0), we get:

$$D_1 a_1 = N_{11} a_1 + N_{12}\Phi_1$$
$$D_1\Phi_1 = N_{21} a_1 + N_{22}\Phi_1, \tag{49}$$

where

$$N_{11} = -\frac{1}{2}\alpha_0 - \mu_0\left(\frac{3}{8}a^2 + B^2\right)$$
$$+ \left[-\kappa_0\left(aB^3 - 3\omega^2 aB^3\right) - 10\lambda_0 aB^3\right]\sin\Phi$$
$$N_{12} = \mu_0\omega B^3\sin\Phi + \left[-\xi_0\omega^2 B^3 - \gamma_0 B^3\right.$$
$$- \kappa_0\left(\frac{1}{2}a^2 B^3 - \frac{3}{2}\omega^2 a^2 B^3 - \omega^2 B^5\right)$$
$$\left.+ \frac{1}{2}\eta_0 fB^2 - \lambda_0\left(5a^2 B^3 + 5B^5\right)\right]\cos\Phi$$
$$N_{21} = \frac{1}{4}\xi_0 a - \kappa_0\left(\frac{1}{4}a^3 + \frac{3}{2}aB^2\right)$$
$$- \lambda_0\left(\frac{5}{4}a^3 - \frac{25}{2}aB^2\right)$$
$$- \frac{3}{4}\gamma_0 a - \frac{1}{a^2}\mu_0\omega B^3\sin\Phi$$
$$+ \frac{1}{a}\left[-\kappa_0\left(aB^3 - 3\omega^2 aB^3\right) - 10\lambda_0 aB^3\right]\cos\Phi$$
$$- \frac{1}{a^2}\left[-\xi_0\omega^2 B^3 - \gamma_0 B^3 + \frac{1}{2}\eta_0 fB^2\right.$$
$$- \kappa_0\left(\frac{1}{2}a^2 B^3 - \frac{3}{2}\omega^2 a^2 B^3 - \omega^2 B^5\right)$$
$$\left.- \lambda_0\left(5a^2 B^3 + 5B^5\right)\right]\cos\Phi$$
$$N_{22} = \frac{1}{a}\mu_0\omega B^3\cos\Phi$$
$$+ \frac{1}{a}\left[-\xi_0\omega^2 B^3 - \gamma_0 B^3 + \frac{1}{2}\eta_0 fB^2\right.$$
$$- \kappa_0\left(\frac{1}{2}a^2 B^3 - \frac{3}{2}\omega^2 a^2 B^3 - \omega^2 B^5\right)$$
$$\left.- \lambda_0\left(5a^2 B^3 + 5B^5\right)\right]\sin\Phi.$$

Finally, the characteristic equation of (49) is Eq. (21).

Appendix C: Subharmonic resonances

Under the condition of order 5 subharmonic resonance, by canceling the resonant terms and after transformation, we obtain:

$$D_1 a = -\frac{1}{2}\alpha_0 a - \mu_0\left(\frac{1}{8}a^3 + aB^2\right)$$
$$- \frac{1}{16}\left[\kappa_0(2\omega - 3) + 5\lambda_0\right]a^4 B\sin\Phi \tag{50}$$

and

$$D_1\Phi = \sigma + 5\xi_0\left(\frac{1}{8}a^2 + \omega^2 B^2\right)$$
$$- 5\lambda_0\left(\frac{5}{16}a^4 - \frac{25}{4}a^2B^2 + 15B^4\right)$$
$$_5\kappa_0\left(\frac{1}{16}a^4 + \frac{3}{4}a^2B^2 + \frac{3}{4}\omega^2 a^2 B^2 + 3\omega^2 B^4\right) \quad (51)$$
$$- 5\gamma_0\left(\frac{3}{8}a^2 + 3aB^2\right)$$
$$+ \frac{5}{2}\eta_0 fB - \frac{5}{16}\left[\kappa_0(2\omega - 3) + 5\lambda_0\right]a^3 B\cos\Phi,$$

with $\Phi = \sigma T_1 - 5\theta$. The amplitudes of oscillations for order 5 subharmonic resonance verify Eq. (22).

The phase in this case is

$$\Phi_0 = \arctan\left(\frac{P_n}{P_d}\right), \quad (52)$$

where

$$P_n = -8\alpha_0 a_0 - \mu_0(2a_0^3 + 16a_0 B^2)$$
$$P_d = \frac{\sigma a}{5} + \xi_0\left(\frac{1}{8}a^3 + \omega^2 aB\right) - \gamma_0\left(\frac{3}{8}a^3 + 3aB^2\right)$$
$$- \kappa_0\left(\frac{1}{16}a^5 + \frac{3}{4}a^3 B^2 + \frac{3}{4}\omega^2 a_0^2 B^2 + 3\omega^2 a_0 B^4\right)$$
$$- \lambda_0\left(\frac{5}{16}a_0^5 - \frac{25}{4}a_0^3 B^2 + 15a_0 B^4\right) + \frac{1}{2}\eta_0 fB.$$

Let us now study the stability of the amplitudes of oscillations. Indeed, using the solution (34) and taking the linear form of (50) and (51) around (a_0, Φ_0), we obtain:

$$D_1 a_1 = P_{11} a_1 + P_{12}\Phi_1 \quad (53)$$

$$D_1\Phi_1 = P_{21} a_1 + P_{22}\Phi_1, \quad (54)$$

with

$$P_{11} = -\frac{1}{2}\alpha_0 - \mu_0\left(\frac{3}{8}a^2 + B^2\right)$$
$$- \frac{1}{4}\left[\kappa_0(2\omega - 3) - 5\lambda_0\right]a_0^3 B\sin\Phi,$$
$$P_{12} = -\frac{1}{16}\left[\kappa_0(2\omega - 3) + 5\lambda_0\right]a^4\cos\Phi$$
$$P_{21} = -5\frac{5}{4}\xi_0 a - 5\kappa_0\left(\frac{1}{4}a^3 + \frac{3}{2}aB^2 + \frac{3}{2}\omega^2 aB^2\right)$$
$$- \frac{15}{4}\gamma_0 a - 5\lambda_0\left(\frac{5}{4}a^3 - \frac{25}{2}aB^2\right)$$
$$- \frac{15}{16}\left[\kappa_0(2\omega - 3) + 5\lambda_0\right]a^2 B\cos\Phi,$$
$$P_{22} = \frac{5}{16}\left[\kappa_0(2\omega - 3) + 5\lambda_0\right]a^3 B\sin\Phi.$$

The characteristic equation of (53) and (54) is Eq. (23).

Finally, the second part of this appendix concerns the order 3 subharmonic resonance. Using the condition of this resonance and Eq. (17), We get

$$D_1 a = -\frac{1}{2}\alpha_0 a - \mu_0\left(\frac{1}{8}a^3 + aB^2\right)$$
$$+ \frac{1}{4}\mu_0 a^2 B\cos\Phi + \left[\xi_0\left(\frac{1}{2}\omega a^2 B - \frac{1}{4}a^2 B\right)\right.$$
$$- \kappa_0\left(\frac{1}{4}a^4 B + \frac{3}{2}\omega a^2 B^3 + \frac{3}{8}a^4 B + \frac{3}{4}\omega^2 a^2 B^3\right)$$
$$\left. - \frac{3}{4}\gamma_0 a^2 B - \lambda_0\left(\frac{5}{4}a^4 B + \frac{15}{2}a^2 B^3\right) + \frac{1}{2}\eta_0 fa^2\right]\sin\Phi$$
$$(55)$$

and

$$D_1\Phi = \sigma + 3\xi_0\left(\frac{1}{8}a^2 + \omega^2 B^2\right)$$
$$- 3\kappa_0\left(\frac{1}{16}a^4 + \frac{3}{4}a^2 B^2 + \frac{3}{4}\omega^2 a^2 B^2 + 3\omega^2 B^4\right)$$
$$- 3\gamma_0\left(\frac{3}{8}a^2 + 3B^2\right) - \frac{3}{4}\mu_0 aB\sin\Phi$$
$$- 3\lambda_0\left(\frac{5}{16}a^4 - \frac{25}{4}a^2 B^2 + 15B^4\right) + \frac{3}{2}\eta_0 fB$$
$$+ 3\left[\xi_0\left(\frac{1}{2}\omega aB - \frac{1}{4}aB\right)\right.$$
$$- \kappa_0\left(\frac{1}{4}a^3 B + \frac{3}{2}\omega aB^3 + \frac{3}{8}a^3 B + \frac{3}{4}\omega^2 aB^3\right)$$
$$\left. - \frac{3}{4}\gamma_0 aB - \lambda_0\left(\frac{5}{4}a^3 B + \frac{15}{2}aB^3\right) + \frac{1}{8}\eta_0 fa\right]\cos\Phi,$$
$$(56)$$

with $\Phi = \sigma T_1 - 3\theta$. Hence the equation of order 3 subharmonic resonance is Eq. (24).

The phase Φ for this resonance is given by

$$\Phi = \arctan\left[\frac{16S_6 S_7 - 4\mu_0 a_0^2 B S_8}{16S_5 S_8 + 12\mu_0 a_0^2 B S_6}\right], \quad (57)$$

where

$$S_5 = \xi_0\left(\frac{1}{2}\omega a^2 B - \frac{1}{4}a^2 B\right) - \frac{3}{4}\gamma_0 a^2 B$$
$$- \lambda_0\left(\frac{5}{4}a^4 B + \frac{15}{2}a^2 B^3\right) + \frac{1}{8}\eta_0 fa^2$$
$$- \kappa_0\left(\frac{1}{4}a^4 B + \frac{3}{2}a^2 B^3 + \frac{3}{8}a^4 B + \frac{3}{4}\omega^2 a^2 B^3\right),$$
$$S_6 = \frac{1}{2}\alpha_0 a_0 + \mu_0\left(\frac{1}{8}a_0^3 + a_0 B^2\right),$$
$$S_7 = 3S_5,$$
$$S_8 = -a\sigma - 3\xi_0\left(\frac{1}{8}a^3 + \omega^2 a_0 B^2\right)$$
$$+ 3\kappa_0\left(\frac{1}{16}a^5 + \frac{3}{4}\omega^2 a^3 B^2 + 3\omega^2 aB^4 + \frac{3}{4}a^3 B^2\right)$$
$$+ 3\gamma_0\left(\frac{3}{8}a^3 + 3aB^2\right) + \frac{3}{2}\eta_0 faB$$
$$+ 3\lambda_0\left(\frac{5}{16}a^5 - \frac{25}{4}a^3 B^2 + 15aB^4\right).$$

Finally, let us study the stability of the amplitudes of oscillations. Indeed, using the solution (34) and taking the linear form of (55) and (56) around (a_0, Φ_0), we obtain:

$$D_1 a_1 = Q_{11} a_1 + Q_{12} \Phi_1, \tag{58}$$

$$D_1 \Phi_1 = Q_{21} a_1 + Q_{22} \Phi_1, \tag{59}$$

with

$$
\begin{aligned}
Q_{11} = & -\frac{1}{2}\alpha_0 - \mu_0\left(\frac{3}{8}a^2 + B^2\right) + \frac{1}{2}\mu_0 aB\cos\Phi \\
& + \left[\xi_0\left(\omega aB - \frac{1}{2}aB\right) - \lambda_0(5a^3 B + 15aB^3)\right. \\
& - \kappa_0\left(a^3 B + 3aB^3 + \frac{3}{2}a^3 B + \frac{3}{2}\omega^2 aB^3\right) \\
& \left. -\frac{3}{2}\gamma_0 aB + \frac{1}{4}\eta_0 fa\right]\sin\Phi,
\end{aligned}
$$

$$
\begin{aligned}
Q_{12} = & -\frac{1}{4}\mu_0 a_0^2 \sin\Phi \\
& + \left[\xi_0\left(\frac{1}{2}\omega a_0^2 B - \frac{1}{4}a^2 B\right)\right. \\
& - \kappa_0\left(\frac{1}{4}a^4 B + \frac{3}{2}\omega a^2 B^3 + \frac{3}{8}a^4 B + \frac{3}{4}\omega^2 a^2 B^3\right) - \frac{3}{4}\gamma_0 a^2 B \\
& \left. -\lambda_0\left(\frac{5}{4}a^4 B + \frac{15}{2}a^2 B^3\right) + \frac{1}{8}\eta_0 fa^2\right]\cos\Phi,
\end{aligned}
$$

$$
\begin{aligned}
Q_{21} = & 3\xi_0\left(\frac{1}{4}a\right) - 3\kappa_0\left(\frac{1}{4}a^3 + \frac{3}{2}aB^2 + \frac{3}{2}\omega^2 aB^2\right) + \frac{9}{4}\gamma_0 a \\
& - 3\lambda_0\left(\frac{5}{4}a^3 - \frac{25}{2}aB^2\right) - \frac{3}{4}\mu_0 B\sin\Phi \\
& - 3\left[\xi_0\left(\frac{1}{2}\omega B\frac{1}{4}B\right) - \kappa_0\left(\frac{3}{4}a^2 B\frac{3}{2}\omega B^3 + \frac{9}{8}a^2 B + \frac{3}{4}\omega^2 B^3\right)\right. \\
& \left. +\frac{3}{4}\gamma_0 B - \lambda_0\left(\frac{15}{4}a^2 B + \frac{15}{2}B^3\right) + \frac{1}{8}\eta_0 f\right]\cos\Phi,
\end{aligned}
$$

$$
\begin{aligned}
Q_{22} = & -\frac{3}{4}\mu_0 aB\cos\Phi + -3\left[\xi_0\left(\frac{1}{2}\omega aB - \frac{1}{4}aB\right)\right. \\
& - \kappa_0\left(\frac{1}{4}a^3 B + \frac{3}{2}\omega aB^3 + \frac{3}{8}a^3 B + \frac{3}{4}\omega^2 aB^3\right) \\
& \left. -\frac{3}{4}\gamma_0 aB - \lambda_0\left(\frac{5}{4}a^3 B + \frac{15}{2}aB^3\right) + \frac{1}{8}\eta_0 fa\right]\sin\Phi.
\end{aligned}
$$

The characteristic equation is Eq. (25).

Declarations

Conflict of interest The authors declare that they have no conflict of interest.

References

1. M.R. Geller, W. Kohn, Phys. Rev. Lett. **70**, 3103 (1993)
2. L. Serra, E. Lipparini, Europhys. Lett. **40**, 667 (1997)
3. P. Ring, P. Schuck, *The Nuclear Many-Body Problem* (Springer, New York, 1980)
4. F. Arias de Saavedra, J. Boronat, A. Polls, A. Fabrocini, Phys. Rev. B **50**, 4248 (1994)
5. A. Puente, L. Serra, M. Casas, Zeitschrift für Physik D Atoms Mol. Clust. **31**, 283 (1994)
6. B. Bagchi, S. Das, S. Ghosh, S. Poria, J. Phys. A Math. Theor. **46**, 032001 (2013)
7. B. Bagchi, A. Banerjee, C. Quesne, V.M. Tkachuk, J. Phys. A Math. Gen. **38**, 2929 (2005)
8. V.C. Ruby, M. Senthilvelan, M. Lakshmanan, J. Phys. A Math. Theor. **45**, 382002 (2012)
9. J.F. Cariñena, M.F. Rañada, M. Santander, Rep. Math. Phys. **54**, 285 (2004)
10. J.F. Cariñena, M.F. Rañada, M. Santander, Ann. Phys. **322**, 434 (2007)
11. S.C. y Cruz, J. Negro, L.M. Nieto, Phys. Lett. A **369**, 400 (2007)
12. S.C. y Cruz, J. Negro, L.M. Nieto, J. Phys. Conf. Ser. **128**, 012053 (2008)
13. S.C. y Cruz, O. Rosas-Ortiz, J. Phys. A Math. Theor. **42**, 185205 (2009)
14. S.C. y Cruz, O. Rosas-Ortiz, SIGMA **9**, 004 (2013)
15. S. Ghosh, S.K. Modak, Phys. Lett. A **373**, 1212 (2009)
16. A. Venkatesan, M. Lakshmanan, Phys. Rev. E **55**, 5134 (1997)
17. P.M. Mathews, M. Lakshmanan, Q. Appl. Math. **32**, 215 (1974)
18. T.O. Roy-Layinde, U.E. Vincent, S.A. Abolade, O.O. Popoola, J.A. Laoye, P.V.E. McClintock, Philos. Trans. A **379**, 2192 (2021)
19. A. Chudzik, P. Perlikowski, A. Stefanski, T. Kapitaniak, Int. J. Bifur. Chaos **21**, 1907 (2011)
20. V. Kamdoum Tamba, S.T. Kingni, G.F. Kuiate, H.B. Fotsin, P.K. Talla, Pramana J. Phys. **91**, 0012 (2018)
21. T. Kroetz, J.S.E. Portela, R.L. Viana, Int. J. Bifur. Chaos **28**, 1830031 (2018)
22. C.H. Miwadinou, A.V. Monwanou, A.L. Hinvi, A.A. Koukpemedji, C. Ainamon, J.B. Chabi Orou, Int. J. Bifur. Chaos **26**, 1650085 (2016)
23. C.H. Miwadinou, A.V. Monwanou, A.L. Hinvi, J.B. Chabi Orou, Pramana J. Phys. **93**, 80 (2019)
24. C.H. Miwadinou, A.V. Monwanou, A.V. Hinvi, J.B. Chabi Orou, Chaos Solitons Fractals **113**, 89 (2018)
25. C.H. Miwadinou, A.V. Monwanou, A.A. Koukpemedji, Y.J.F. Kpomahou, J.B. Chabi Orou, Int. J. Bifur. Chaos **28**, 1830005 (2018)
26. D.L. Olabodé, C.H. Miwadinou, V.A. Monwanou, J.B. Chabi Orou, Phys. Scr. **93**, 085203 (2018)
27. C.H. Miwadinou, V.A. Monwanou, J. Yovogan, L.A. Hinvi, P.R. Nwagoum Tuwa, J.B. Chabi Orou, Chin. J. Phys. **56**, 1089 (2018)
28. C.H. Miwadinou, L.A. Hinvi, A.V. Monwanou, J.B. Chabi Orou, Nonlinear dynamics of a ϕ^6-modified Duffing oscillator: resonant oscillations and transition to chaos. Nonlinear Dyn. **88**, 97–113 (2017)
29. M. Siewe Siewe, H. Cao, M.A.F. Sanjuán, Chaos Solitons Fractals **41**, 772 (2009)
30. M.I. Evstifeev, A.S. Kovalev, D.P. Eliseev, Gyroscopy Navig. **5**, 174 (2014)
31. Z. Iskakov, K. Bissembayev, Mech. Sci. **10**, 529 (2019)
32. R.G. Wang, Y. Chen, G.W. Cai, Adv. Mat. Res. **139**, 2381 (2010)
33. A.V. Monwanou, A.A. Koukpémèdji, C. Ainamon, P.R. Nwagoum Tuwa, C.H. Miwadinou, J.B. Chabi Orou, Complexity **2020**, 8823458 (2020)
34. G.D. Leutcho, S. Jafari, I.I. Hamarash, J. Kengne, Z. Tabekoueng Njitacke, I. Hussain, Chaos Solitons Fractals **134**, 109703 (2020)
35. G.D. Leutcho, A.J.M. Khalaf, Z. Tabekoueng Njitacke, T. Fonzin Fozin, J. Kengne, S. Jafari, I. Hussain, Chaos **30**, 033112 (2020)
36. Z. Tabekoueng Njitacke, D.I. Sami, N. Tsafack, J. Kengne, Neural Comput. Appl. **33**, 6733–6752 (2021)
37. Z. Tabekoueng Njitacke, R.L. Tagne Mogue, G.D. Leutcho, T. Fonzin Fozin, J. Kengne, Int. J. Electron. **108**, 7 (2021)
38. K. Rajagopal, S. Takougang Kingni, G.H. Kom, V.-T. Pham, A. Karthikeyan, S. Jafari, J. Korean Phys. Soc. **77**, 145 (2020)

39. G.D. Leutcho, J. Kengne, Chaos Solitons Fractals **113**, 275 (2018)
40. Z. Tabekoueng Njitacke, I.D. Sami, J. Kengne, A. Nguomkam Negou, G.D. Leutcho, Eur. Phys. J. Spec. Top. **229**, 1133 (2020)
41. G.D. Leutcho, J. Kengne, T. Fonzin Fozin, K. Srinivasan, Z. Njitacke Tabekoueng, S. Jafari, M. Borda, J. Comput. Nonlinear Dyn. **15**, 051004 (2020)
42. C. Hayashi, *Oscillations in Physical Systems* (McGraw-Hill, New York, 1964)
43. A.H. Nayfey, D.T. Mook, *Nonlinear Oscillations* (Wiley, New York, 1979)
44. D.B. Marghitu, *Mechanical Engineer's Handbook* (Academic Press Series in Engineering, New York, 2001)
45. T. Roskilly, R. Mikalsen, *Marine Systems Identification, Modeling, and Control* (Oxford, Kidlington, England, 2015)